cryo

Review

Research Progress of Epoxy-Based Composites for Insulating Encapsulation of Superconducting Magnets

Shen Zhao, Zhicong Miao, Zhixiong Wu, Rongjin Huang and Laifeng Li

Special Issue
Low Temperature Physics, Pioneer of Chinese Low Temperature Physics and Cryogenics—In Memory of Prof. Dr. Chaosheng Hong (C.S. Hung)

Edited by
Prof. Dr. Laifeng Li, Prof. Dr. Chuanjun Huang and Dr. Feng Feng

MDPI

https://doi.org/10.3390/cryo2010002

cryo

MDPI

Review

Research Progress of Epoxy-Based Composites for Insulating Encapsulation of Superconducting Magnets

Shen Zhao [1,2], Zhicong Miao [1,*], Zhixiong Wu [1,*], Rongjin Huang [1,2] and Laifeng Li [1]

[1] State Key Laboratory of Cryogenic Science and Technology, Technical Institute of Physics and Chemistry, Chinese Academy of Sciences, Beijing 100190, China
[2] Center of Materials Science and Optoelectronics Engineering, University of Chinese Academy of Sciences, Beijing 100049, China
* Correspondence: miaozhicong@mail.ipc.ac.cn (Z.M.); zxwu@mail.ipc.ac.cn (Z.W.)

Abstract

Epoxy-based composites are crucial insulating and structural materials for superconducting magnets, providing mechanical strength, winding fixation, and heat transfer. However, future superconducting devices with higher integration and power will place even higher demands on their toughness, thermal conductivity, electrical insulation, and radiation resistance at low temperatures. Otherwise, problems such as cracking, detachment, and low heat dissipation efficiency will arise, which may lead to quenching of low-temperature superconductors (Nb_3Sn, NbTi) and a decline in the performance of high-temperature superconductors (YBCO). Research focuses on summarizing the recent progress in modifying epoxy resin to address these issues. The current strategies include formula optimization using mixed curing and toughening agents to enhance mechanical properties, incorporating functional fillers to improve cryogenic thermal conductivity and reduce the coefficient of thermal expansion. Studies also evaluate cryogenic electrical insulation performance (DC breakdown strength, flashover voltage) and radiation resistance under cryogenic conditions. These advancements aim to develop reliable epoxy composites, ensuring the stability and safety of superconducting magnets in applications such as particle accelerators and fusion reactors.

Keywords: epoxy; insulating material; superconducting magnet; cryogenic properties

1. Introduction

Epoxy resin is widely used as an insulating material due to its excellent bonding properties, high mechanical strength, good electrical insulation characteristics, and controllable curing process [1,2]. The cured epoxy resin can form highly crosslinked three-dimensional networks that exhibit a high modulus and dimensional stability [3,4]. These advantages make epoxy resin a natural choice for highly demanding electrical insulation applications.

In superconducting magnet systems, insulating encapsulation is a critical component for ensuring stable operation, which primarily serves several functions: First, it ensures electrical isolation between conductors, preventing electrical shorting [5,6]. Second, it provides structural integrity by transferring stresses between the coil and support structures [7]. Third, it acts as a protective encapsulant, maintaining the coil geometry and securing the magnet from environmental damage [8,9]. Therefore, a reliable insulation system directly impacts the reliability, lifespan, and safety of superconducting magnets.

Due to the extreme operation environments, insulating materials must withstand immense electromagnetic stresses, fatigue loads from thermal cycling, and potentially

Academic Editor: Arman Siahvashi

Received: 12 October 2025
Revised: 10 December 2025
Accepted: 31 December 2025
Published: 5 January 2026

high-energy neutron irradiations in nuclear fusion devices [10,11]. However, epoxy resin matrices exhibit several intrinsic shortcomings that limit their performance under these extreme conditions: the highly crosslinked network structure, while beneficial for the modulus and dimensional stability, makes epoxy inherently brittle, showing limited elongation and poor resistance to crack propagation at cryogenic temperatures [12,13]; thermal contraction mismatch between the resin matrix and reinforcing fibers or inorganic fillers generates significant internal stresses during thermal cycles, often leading to microcracking or interfacial debonding [14,15]; the inherent low thermal conductivity makes it detrimental to countering super conductor quenching caused by localized heat accumulation [16]; surface flashover or internal electrical treeing structures are prone to occur under high-voltage environments, leading to electrical breakdown and insulation failure [17]; and finally, under long-term irradiation, epoxy might undergo chain scission and crosslinking failures, leading to significant degradations in mechanical properties and insulating performances [18,19]. These factors directly threaten the reliability of coil insulation.

At present, glass fiber-reinforced epoxy composite materials combined with polyimide films are most commonly used as insulating materials, particularly for turn insulation, interlayer insulation, and ground insulation in large fusion magnets [20,21]. Glass fibers can effectively distribute loads, enhance dimensional stability, and inhibit crack propagation, while reducing the effective stress on the brittle resin matrix [22,23]. Polyimide films, such as Kapton, are often integrated with glass fiber to enhance dielectric stability and resistance to partial discharge [24]. More recently, inorganic nanoparticles (e.g., silica, alumina, hexagonal boron nitride) have been incorporated to improve mechanical strength, enhance resin–fiber interfacial adhesion, reduce thermal contraction, and increase dielectric breakdown strength [25–27]. Hybrid approaches, combining nano-scale fillers with traditional fiber reinforcements, offer further optimization [28,29]. In terms of chemical modification, modified resin formulations such as cyanate ester/epoxy blends have been designed to resist irradiation-induced embrittlement while preserving processability [30]. These approaches aim to design advanced epoxy composites that can balance electrical insulation, mechanical strength and toughness, thermal compatibility, and radiation resistance at cryogenic temperatures. The cryogenic property requirements and modification methods for epoxy-based insulation materials are shown in Figure 1.

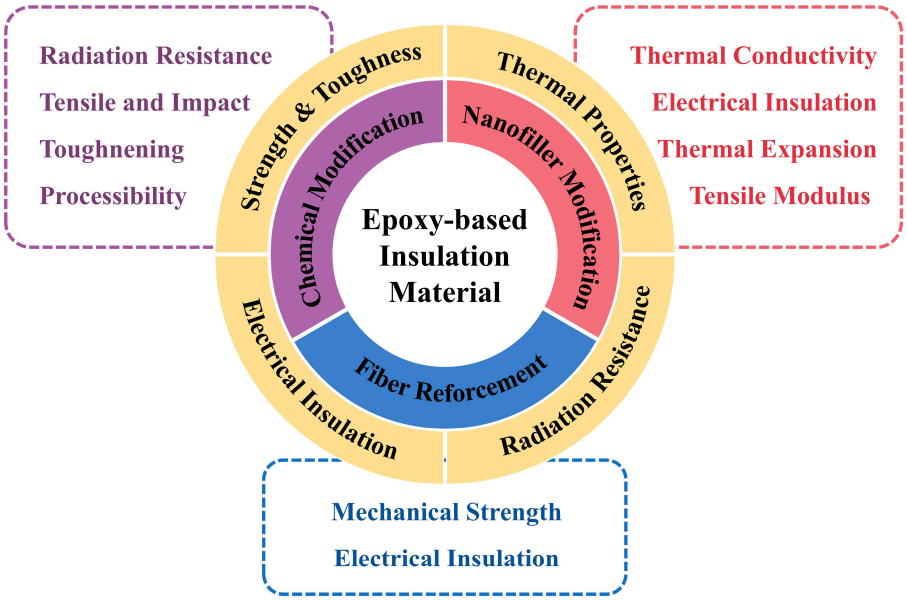

Figure 1. Schematic illustration of the cryogenic property requirements and modification methods for epoxy-based insulation materials.

In this review article, we systematically summarize the cryogenic performance of epoxy composites as insulating encapsulation materials for superconducting magnets and the corresponding strategies for their improvement. It focuses on analyzing their mechanical behavior, thermal properties, electrical insulation performance, and radiation resistance under cryogenic conditions. Additionally, the current primary modification techniques are categorized and critically discussed. Hopefully, this work fills a gap in the summary of cryogenic performances of epoxy-based composites and provides a theoretical basis and technical reference for the future design and application of insulating materials in superconducting magnets.

2. Cryogenic Property Enhancement of Epoxy Resin

2.1. Mechanical Properties

Insulation materials face immense electromagnetic and thermal stresses during magnet operation. The International Thermonuclear Experimental Reactor (ITER) requires a minimum ultimate tensile strength (UTS) of 600 MPa and a minimum interlaminar shear strength (ILSS) of 60 MPa for magnet insulation encapsulation materials [31–33]. However, pure epoxy resin lacks sufficient strength to meet these mechanical requirements. Therefore, glass fiber is employed as a reinforcing material, which not only enhances the mechanical strength and toughness of the epoxy matrix but also offer excellent durability, insulating properties, and thermal stability [34]. Researchers have characterized the cryogenic mechanical properties of different glass fiber-reinforced plastics (GFRP).

Wu and his colleagues evaluated the mechanical properties of vacuum bag-processed GFRP at 77 K, including short-beam strength (SBS), tensile strength, and fatigue fracture strength after 30,000 cycles [35]. The transverse and longitudinal SBS values of the GFRP were 125 and 104 MPa, respectively, with a UTS of 759 and 638 MPa. After 30,000 cycles of 400 MPa stress loading, the UTS of GFRP remained at 518 MPa. Without considering other factors, these strength values of GFRP have all already met ITER requirements. However, in practical superconducting applications, high-dose irradiation will cause molecular chain breakage in epoxy resins, leading to significant deterioration in the tensile strength and toughness. An effective solution is to modify the resin matrix by introducing resins with superior radiation resistance, such as cyanate ester. Hummer et al. investigated the static tensile and interlaminar shear strengths at 77 K of boron-free glass fiber in commercial epoxy, cyanate ester, and epoxy/cyanate ester/polyimide/bismaleimide blend matrix systems before and after neutron irradiation to a fluence of 1×10^{22} m^{-2} at ambient temperature (E > 0.1 MeV) [36,37]. It was found that commercial epoxy systems exhibited significant mechanical degradation post-irradiation, with UTS (0° direction) decreasing from 800–950 MPa to 550–900 MPa, accompanied by poor fatigue performance. Pure cyanate ester systems (CTD-403) demonstrated excellent radiation resistance, while the blended system (CTD-x series) exhibited the best overall mechanical properties: post-irradiation UTS remained at 870–1060 MPa, ILSS at 62–98 MPa, and the tensile fatigue limit at 250–300 MPa. The use of cyanate ester or cyanate ester-containing systems can maintain high mechanical strength comparable to epoxy systems while significantly enhancing the radiation resistance of resins, making it a viable solution for insulating material.

Additionally, increasing the functionality of epoxy resin can enhance its radiation resistance, but this typically compromises its processability. Wu et al. investigated the effects of different epoxy matrices (DGEBF, TGPAP) and modifiers (IPBE, HTDE-2) on the processing properties and radiation resistance of GFRP composites [38]. It was shown that compared to DGEBF-based epoxy resins, TGPAP-based epoxy resins exhibited lower initial viscosities and longer working life. The ILSS of TGPAP-based composites was lower than that of DGEBF-based composites under non-irradiated conditions. However, the

TGPAP-based system demonstrated superior radiation resistance, with ILSS remaining higher than or at least equal to the non-irradiated level after ^{60}Co γ-ray irradiation at ambient temperature (radiation dose rate was 300 Gy/min and the maximum dose was 10 MGy). In contrast, the DGEBF-based system exhibited a 57% decrease in ILSS after irradiation. For modifiers, HTDE-2 and IPBE can enhance the ILSS of composites prior to irradiation, but reduce the irradiation resistance. It revealed that GFRP prepared from highly functional epoxy resin with the assistance of specific modifiers can achieve a balance between radiation resistance and processability.

Combining fiber reinforcement with nanofillers offers a new approach. Bao et al. utilized AlN nanoparticles to enhance the mechanical properties of GFRP via the VARTM impregnation method [39]. AlN nanopowder was deposited onto glass fibers and subsequently incorporated into a cyanate ester/epoxy matrix. It was demonstrated that the SBS of the reinforced composite at 77 K increased by 6.32% compared to the original GFRP. The values of cryogenic mechanical properties of these GFRPs are summarized in Table 1. Among the listed materials, systems containing cyanate esters exhibit the highest tensile and shear strengths, together with minimal degradation after neutron irradiation, indicating that they represent one of the most suitable resin candidates for magnet impregnation.

Table 1. Summary of the mechanical properties of GFRP at 77 K compared with ITER requirements.

Resin	TS (MPa)	ILSS (MPa)	Ref.
ITER requirements	>600	>60	[31–33]
Epoxy	759	125	[35]
Epoxy (EU3)	882	68	[36]
CE (CTD-403)	894	108	[36]
CE/epoxy (CTD-422)	1043	88	[36]
CE/epoxy/bismaleimide (CTD-10x)	999	-	[36]
CE/epoxy/polyimide (CTD-7x)	1113	94	[36]
Epoxy (DGEBF)	-	80–82	[38]
Epoxy (TGPAP)	-	58–66	[38]
Epoxy (DGEBF)/CE (DCBE)/AlN (21.07 wt%)	-	90	[39]

A similar material selection can be observed in high-energy physics applications. For example, CERN has long employed CTD-101K—a DGEBA/anhydride epoxy system—to impregnate superconducting coils for the Large Hadron Collider (LHC) and the ongoing High-Luminosity LHC upgrade, due to its stable performance under cryogenic temperatures and its relatively low chain-scission rate under ionizing radiation [40]. More recently, the improved resin formulation POLAB Mix (CTD-101K + DY040), incorporating a polyether modifier, has been introduced to enhance cryogenic toughness [41]. These developments highlight that, in addition to high strength, reliable resistance to cryogenic embrittlement is increasingly critical for large-scale superconducting magnet systems.

Epoxy-based insulating materials exhibit low elongation at break and weak impact resistance, making them susceptible to failure when subjected to localized high-intensity stresses [42,43]. Consequently, researchers have explored various modifiers to enhance the tensile performance and toughness of epoxy resins.

One approach involves introducing insulating inorganic nano fillers for mechanical enhancement. Fan et al. investigated the effect of graphene oxide (GO) with varying degrees of oxidation on the cryogenic mechanical properties of GO/epoxy nanocomposites [44]. It was found that the degree of oxidation enhanced the dispersion and the interfacial interaction with epoxy resin. At a low GO loading of 0.10 wt%, the GO/epoxy nanocomposite exhibited the highest tensile strength of 123.2 MPa (77 K), representing an increase of 14%

over pure epoxy resin. Jin et al. synthesized an EP/CPN-CuO nanocomposite with high tensile strength and fracture toughness by using α-cyclodextrin (α-CD) for anchoring [45]. α-CD anchored flexible linear polymers attached to the surface of CuO nanorods, which effectively prevented polymer chain curling and significantly enhanced the chemical bonding between the epoxy resin and CuO. It was demonstrated that the tensile strength, Young's modulus, and fracture toughness of EP/CPN-CuO represented improvements of 67.4%, 10.8%, and 100.7%, respectively, compared to pure epoxy resin. Although nanofiller modification has proven effective in enhancing the mechanical properties of epoxy resins, issues of the inherent insulation of the fillers and the influence of loading rate must be considered.

Chemical modification is another effective method for toughening epoxy resins, which does not significantly alter the insulation properties or processability. One common strategy is to introduce flexible structures into epoxy resins. Yang and colleagues utilized two types of flexible diamine (D-230 and D-400) to toughen DGEBA epoxy resin [46]. The mechanical property differences in the modified epoxy resin at room temperature and 77 K were investigated, including tensile properties and Charpy impact strength. The results indicate that the addition of flexible diamines may reduce the tensile strength at room temperature but increase the tensile strength at 77 K. The reduction in tensile strength is attributed to the increased chain length introduced by the flexible diamines, which lowers the crosslink density of the epoxy. However, due to the low-temperature shrinkage effect, the chain length shortens at 77 K, while the flexible diamines effectively reduce internal stresses within the epoxy, which ultimately enhances tensile strength. Additionally, stress relaxation from the flexible diamine molecular chains enhances both elongation at break and impact strength at both room temperature and 77 K. Mishra et al. prepared polyhedral oligomeric silsesquioxane (POSS)/epoxy composites via mechanical mixing [47]. It was revealed that incorporating 5 wt% POSS could increase fracture toughness at 77 K by 40% compared to the pure epoxy resin. The addition of POSS led to the formation of deformable regions instead of the changes in free volume inside the molecular network. Wu et al. evaluated the mechanical properties of the DGEBA/DETDA system with two hydroxyl-terminated polyurethanes (HTPU1 and HTPU2) at room temperature and 77 K [48], by studying modifiers with different molecular weights, to reveal the influence of phase structure on overall resin performance. It was found that the introduction of HTPU1 and HTPU2 successfully yielded two distinct phase states in composites: a homogeneous phase and a sea–island structure. The homogeneous phase demonstrated more pronounced enhancement effects on impact and tensile properties, while the sea–island structure exhibited better retention in the glass transition temperature of the matrix.

In addition to using flexible molecular chains as modifiers, researchers have discovered that hyperbranched structures can effectively enhance the toughness of epoxy resins as well. Yang et al. employed a hydroxyl-functionalized hyperbranched polymer (H30) to enhance the mechanical properties of DGEBA epoxy resin at 77 K [49]. It was demonstrated that adding an appropriate amount of H30 simultaneously improved tensile strength, fracture ductility, and impact strength at 77 K. By introducing 10 wt% H30, the maximum tensile strength and impact strength at 77 K represented a 17.7% and 26.3% improvement over pure epoxy resin, respectively. Additionally, the fracture strain at 77 K increased continuously with rising H30 content. These are mainly attributed to the reduction in internal stress after the introduction of soft flexible groups of H30 into the brittle epoxy network. Interestingly, the impact strength of the modified system at 77 K was not lower than that at room temperature. The flexible ester segments in H30 remain unfrozen at 77 K and still can dissipate the impact energy by segmental motion. Zhao et al. further investigated the effect of free volume from hyperbranched structures on the mechanical properties of epoxy-based composites [50]. Through positron annihilation lifetime measurements,

nano-scaled free-volume holes were characterized. Subsequently, composites with smaller free-volume holes exhibited superior impact and compression properties. Concurrently, at 77 K, the impact and tensile properties of the composites showed a positive correlation with the fraction of free-volume holes. Zhao et al. prepared HBP-GO/EP composites by grafting GO with hyperbranched polymers (HBP) [51]. HBP-GO were uniformly dispersed and firmly bonded with the epoxy matrix through strong chemical interactions, significantly improving the thermal performance of the composites. With only 0.2 wt% HPB-GO loading, significant improvements of 58.53%, 68.32%, and 57% were observed in impact strength, tensile strength, and compressive strength, respectively, compared to pure epoxy resin. Subsequently, the authors further employed a similar approach to perform hyperbranched grafting on BN and prepared HPB-BN/EP composites [52]. As a result, the maximum tensile and impact strengths of 4 wt% HPB-BN/EP increased by 72% and 135% at 77 K, respectively, compared to pure epoxy. These studies demonstrate that hyperbranching modification of epoxy resins is one of the effective means for mechanical property enhancement.

The summary of the mechanical properties of the above modified epoxy-based composites is shown in Table 2. In general, nanofiller reinforcement effectively improves the tensile modulus; however, it is less effective than chemical modification in enhancing elongation at break and impact resistance, and it may also adversely affect the processing properties of the resin. Therefore, chemical modification should be considered the primary approach for toughening of epoxy resins.

Table 2. Summary of the mechanical properties of epoxy-based composites at 77 K toughened by different modification methods.

Resin	Modifier (Content)	Tensile Strength (MPa)	Tensile Modulus (GPa)	Elongation at Break (%)	Impact Strength (kJ/m^2)	Fracture Toughness (MPa·m$^{1/2}$)	Ref.
Epoxy (DGEBA)	GO (0.1 wt%)	108	5.7	8.2	-		[44]
Epoxy (DGEBA)	CPN-CuO (2 wt%)	111.40	6.67	1.63	-	2.69	[45]
Epoxy (DGEBA)	Flexible diamine D-230 (49 wt%)	107.6	5.11	2.18	21.62		[46]
Epoxy (DGEBA)	Flexible diamine D-400 (49 wt%)	108.02	5.23	2.03	16.56		[46]
Epoxy (DGEBF)	POSS (5 wt%)	-	-	-	-	2.3	[47]
Epoxy (DGEBA/DETDA)	HTPU (5 phr)	161.67	6.89	2.58	-	-	[48]
Epoxy (DGEBA)	H30 (10 wt%)	115.6	3.8	3.1	32.0		[49]
Epoxy (DGEBA)	HPB (7.5 wt%)	74.37	5.7	-	17.2	-	[50]
Epoxy (DGEBA)	HPB-GO (0.2 wt%)	86	-	-	18	-	[51]
Epoxy (DGEBA)	HPB-BN (4 wt%)	96	-	-	24	-	[52]

Multi-scale modeling techniques, ranging from molecular dynamics to continuum-level micromechanics models, have been employed for predicting composite behavior and establishing structure–property relationships. Elmasry et al. provided a comprehensive overview of the recent progress in multi-scale modeling of nanocomposites [53]. Through modeling different resin formulations and composite structures, guidance for composite optimization can be provided more efficiently.

2.2. Thermal Properties

Beyond mechanical properties, it is equally critical to understand the thermal properties of insulation materials. Thermal expansion properties affect the dimensional stability, strength, and mechanical compatibility of insulation material [54,55]. Significant differences in thermal expansion coefficients between the magnet and the insulation can lead to severe thermal stress accumulation during thermal cycling, ultimately causing insulation encapsulation failure [56]. Furthermore, due to the freezing of molecular chains at cryogenic temperatures, epoxy resin exhibits extremely low thermal conductivity [57,58]. Once thermal accumulation occurs, it may not only accelerate the aging of the epoxy resin but also cause uncontrolled magnet temperature, severely compromising the operational stability and reliability of superconducting magnets.

Researchers have tested the thermal properties of different fiber-reinforced epoxy composites. Wu et al. investigated the thermal behavior of glass fiber-reinforced IPBE/TGPAP epoxy-based composites with DETDA as curing agent [59]. The thermal conductivity of the composite ranges from 0.24 to 0.44 W/(m·K) between 77 and 300 K. Moreover, it was indicated that the thermal properties and chemical structure of GFRP remained unaffected by ^{60}Co gamma radiation with a dose rate of 100 Gy/min and a total dose of 1 MGy. Krzak et al. evaluated the thermal properties of carbon fiber, basalt fiber, and glass-fiber reinforced epoxy resin under cryogenic conditions [60]. Thermal conductivity and full-hemispherical emissivity were obtained across a broad temperature range from 5 K to 300 K. Basically, fiber-reinforced epoxy composites exhibit low thermal conductivities at 77 K, typically around 0.25 W/(m·K).

To address this, researchers have explored various approaches, including adding thermal conductive additives, modifying epoxy resins, and enhancing interfacial interactions. The most common approach is to incorporate nanofillers. Bao et al. enhanced GFRP by introducing AlN nanoparticles onto glass fibers via the VARTM immersion absorption method [39]. The results showed an increase in the thermal conductivity and a significant decrease in the thermal expansion coefficient with the addition of aluminum nitride nanopowders. Zhang and colleagues utilized aminopropyltrimethoxysilane-treated boron nitride nanotubes (BNNT-APS) as fillers to prepare epoxy nanocomposites [61]. At a loading of 10 wt%, the nanocomposites exhibited a 650% enhancement in thermal conductivity at both room temperatures and 77 K, with a 20% reduction in CTE. Meanwhile, the nanocomposites maintained a low dielectric constant and dielectric loss. These results were attributed to the outstanding intrinsic properties of BNNTs, effective surface modification by APS molecules, and low interfacial thermal resistance between BNNTs and matrix. Zhou et al. tested the cryogenic thermal conductivities of AlN/epoxy and SiC/epoxy composites [62]. It was found that compared to pure epoxy resin, the composites exhibited a slower reduction in thermal conductivity with decreasing temperature. Furthermore, the composites showed superior dynamic mechanical properties, dielectric properties, and a lower coefficient of thermal expansion. Zhou et al. utilized the ice-template method to prepare BNNS/nanodiamond (ND) aerogels with three-dimensional (3D) structures, followed by impregnation with epoxy resin to fabricate epoxy composites [63]. BNNS and ND exhibited significant synergistic effects in enhancing thermal conductivity, while the 3D structure endowed the composite with strong thermal anisotropy. As a result, the BNNS/ND/epoxy composite demonstrates a thermal conductivity of 0.67 W/(m·K) at 100 K and a coefficient of thermal expansion (CTE) of 34.4 $\times$ 10^{-6} K^{-1}. Xiang et al. employed α-Si_3N_4 and β-Si_3N_4 as a binary filler to reinforce epoxy resin [64]. It was revealed that the binary fillers could facilitate thermal conduction pathways more effectively than single-filler systems. At a 60 wt% loading, the Si_3N_4/EP composite (α-Si_3N_4:β-Si_3N_4 = 2:8) exhibited a thermal conductivity of 3266% higher than pure epoxy resin at 77 K. While

the average CTE of the Si_3N_4/EP composite dropped to 14.1 × 10^{-6} K^{-1}, representing a 63% reduction.

Chemical modification methods on the thermal properties include utilizing liquid crystal epoxy (LCE) or combining thermally conductive fillers with hyperbranched polymers. Li et al. designed an azomethine-type LCE and combined it with KH-550-modified boron nitride to prepare K-BN/LCE composites [65]. With 30 wt% loading of K-BN, the composites showed a thermal conductivity of 0.50 W/(m·K) at 77 K, which was five times that of pure epoxy resin. Unlike the inherently disordered molecular chain structure within epoxy, the presence of micro-ordered domains in LCE generates an anisotropic structure that reduces phonon scattering and lowers interfacial thermal resistance. On the other hand, the modified BN filler improves its own dispersibility and forms continuous conduction pathways with the micro-ordered domains, enabling efficient heat transfer. The composite also exhibited a maximum CTE reduction of 37.8% while maintaining sufficient shear strength. Hyperbranched modification also effectively enhances the thermal conductivity of epoxy resins due to the reduction in the interfacial thermal resistance between fillers and epoxy. The previously mentioned HPB-GO/EP and HPB-BN/EP composites demonstrated thermal conductivity increases of 80% and 430%, respectively, compared to pure epoxy resin [51,52].

The thermal properties of epoxy-based composites are summarized in Table 3. The thermal conductivity of unmodified fiber-reinforced epoxy resin is approximately 0.25 W/(m·K) at 77 K. With the incorporation of thermally conductive filler, the thermal conductivity can be increased by 100–300%.

Table 3. Summary of the thermal conductivities and coefficient of thermal expansion of epoxy-based composites at cryogenic temperatures.

Resin	Fiber	Nano Filler (Content)	T (K)	T_c (W m^{-1} K^{-1})	CTE (10^{-6}/K)	Ref.
Epoxy (IPBE/TGPAP)	Glass fiber	-	77	0.24	10.07 (fill direction) 12.03 (warp direction) 32.35 (z-direction)	[58]
Epoxy (KEP-1138)	Glass fiber	-	70	0.23	-	[59]
Epoxy (KEP-1138)	Basalt–glass fiber	-	70	0.25	-	[59]
Epoxy (DGEBF)/CE (DCBE)	Glass fiber	AlN (31.62 wt%)	77	0.60	27.2	[39]
Epoxy (DGEBF)	-	BNNT-APS (5 wt%)	77	0.63	36	[60]
Epoxy (DGEBF)	-	AlN (60 wt%)	60	0.20	27.6	[61]
Epoxy (DGEBF)	-	SiC (60 wt%)	60	0.24	23.0	[61]
Epoxy (DGEBF)	-	BNNS/nanodiamond (50.7 wt%)	100	0.67	34.4	[62]
Epoxy (DGEBF)	-	α-Si_3N_4/β-Si_3N_4 (60 wt%)	77	1.09	14.1	[63]
Liquid crystal epoxy	-	BN (30 wt%)	77	0.50	28	[64]
Epoxy (DER-332)	-	HPB-BN (40 wt%)	100	0.93	34	[52]

2.3. Electrical Properties

During the operation of superconducting devices, in addition to the cryogenic environment (77 K or 4.2 K), high voltage, high magnetic field strength (>10 T), strong radiation, and thermal stress concentration are generated, causing the insulation structure to remain in an extremely harsh environment for extended periods [66,67]. The presence of impu-

rities and defects in the insulating material increases the likelihood of partial discharge phenomena, leading to electron avalanches, thermal pulses, and dynamic pulses [68,69]. The concentrated voltage causes breakdown in the microscopic regions around the defects, resulting in the overall electrical breakdown of the material [70]. This not only causes the loss of insulation properties but also leads to a sharp decline in mechanical performance, ultimately causing the superconductor to quench and resulting in severe economic losses and significant safety risks.

Electrical damage is the primary cause of insulation structure degradation, with electrical treeing, electrical breakdown, and surface flashover being the main manifestations of such damage [71,72]. The electrical insulation properties of epoxy in the low-temperature region typically exhibit patterns different from those in the room-temperature to high-temperature range.

The surface flashover voltage of solid materials is usually lower than the breakdown voltage [73]. Therefore, multiple flashovers may occur before electrical breakdown takes place, which can cause irreversible damage to the material surface. Hence, studying flashover at low temperatures is crucial for the stable operation of high-voltage superconducting equipment. Research indicates that the secondary electron emission rate and the cathode electron emission rate are the main factors affecting the surface breakdown strength under vacuum conditions. Jiang et al. built an efficient integrated electrical testing system, which realized a wide-range testing of the electrical performance of epoxy resin from cryogenic to room temperature [74]. The surface flashover of epoxy was investigated, and the Weibull distribution results indicate that the flashover strength of epoxy resin does not increase monotonically with decreasing temperature. It was affected by the work function of the copper electrode and the time scales of the above-process and the sub-process, where both the collision ionization of gas molecules and carrier migration toward the anode become more difficult as temperature decreases. Subsequently, they continued to utilize this equipment to investigate the influence of different types of filler doping on the surface flashover characteristics of epoxy resin at cryogenic temperatures. The study shows that an appropriate amount of filler doping can significantly enhance the flashover strength of epoxy resin at cryogenic temperatures. It is primarily due to the addition of filler creating traps to capture charge carriers and hinder their migration. Moreover, the effectiveness of the fillers varies considerably across different temperature ranges. It was observed that BNNS/EP composites with 1–3 wt% filler content exhibited superior surface flashover performance compared to pure epoxy [75]. Notably, their flashover voltage followed a non-monotonic trend, initially increasing before decreasing as temperatures dropped. In contrast, at the extreme cryogenic temperature of 10 K, the addition of BNNS, regardless of quantity, proved detrimental to the flashover strength. The effectiveness of ZnO nanoparticles was highly temperature-dependent, enhancing the surface flashover characteristics of epoxy nanocomposites solely within the 80 K to 280 K range. In contrast, Al_2O_3/EP composites consistently outperformed pure epoxy across the entire temperature spectrum. The optimal filler content for Al_2O_3 was found to be 1 wt% in the deep cryogenic regime (10 K to 80 K), while 2 wt% yielded the best performance at all other temperatures [76]. The variation in the effect of fillers on the dielectric strength of epoxy-based composite may be related to their intrinsic bandgap and dispersion. The presented work thus offers practical guidance for enhancing epoxy's low-temperature performance. However, it also reveals a more complex physical picture than a simple monotonic dependence. A deeper exploration of the fundamental mechanisms is necessary. Crucially, the influence of the surface gas state under cryogenic conditions must be considered and systematically studied in future work.

During the operation of a superconducting magnet, fluctuations such as local temperature rises may cause a local quench, resulting in a large voltage difference [77,78]. This can

lead to a transient electrical breakdown. Therefore, the electrical breakdown strength of epoxy resin at low temperatures serves as a critical indicator for evaluating the performance of superconducting magnet systems. A study by Wang et al. on glass fiber-reinforced epoxy revealed a significant enhancement in DC breakdown strength at 78 K compared to 300 K, with a 25 kV/mm improvement determined by Weibull analysis. They concluded that the cryogenic conditions freeze the polymer's molecular chains and side branches, which suppresses atomic vibrations, reduces free volume, hinders electron multiplication, and limits charge carrier mobility, thereby collectively increasing the breakdown strength [79]. Adding nano- or micrometer fillers is also one of the main methods to improve the insulation performance of epoxy resins. Lee et al. investigated the low-temperature electrical properties of epoxy resin modified with silica microfillers and alumina and titanium dioxide nanofillers [80]. Through AC withstand voltage tests and partial discharge inception voltage tests, they found that the nanofiller-modified epoxy composites demonstrated higher breakdown strength compared to those with micron-sized fillers in cryogenic environments, while exhibiting similar breakdown voltage characteristics to insulating oil. Jiang et al. investigated the DC breakdown strength and surface potential behavior of epoxy/alumina nanocomposites (with 0, 1, 3, and 5 wt% filler content) under both room temperature and cryogenic conditions [81]. The study revealed that with increasing nanoparticle content, both the DC breakdown strength and initial surface potential exhibited a trend of an initial increase followed by a decrease. Under cryogenic conditions, enhancements in breakdown strength and initial surface potential were also observed. Furthermore, at low temperatures, the incorporation of nanoparticles significantly altered the trap distribution, thereby affecting the dielectric strength. This phenomenon is primarily attributed to reduced space charge accumulation, modified charge carrier mobility, and variations in charge carrier energy within the bulk material. Jia et al. investigated the DC breakdown strength of GFRP incorporated with zinc oxide nanoparticles at both cryogenic and room temperatures [82]. The zinc oxide nanoparticles were modified with a silane coupling agent. The results demonstrated that increasing the content of modified zinc oxide nanoparticles enhanced the DC breakdown strength of GFRP, reaching its maximum at 5 wt% concentration. This improvement is attributed to the fact that the incorporated zinc oxide nanoparticles hinder the electron multiplication process during electrical breakdown. Furthermore, the breakdown strength of the same material at 77 K was found to be higher than that at 300 K, primarily due to the suppressed mobility of chain segments and reduced kinetic energy of charge carriers in the epoxy matrix under cryogenic conditions. Koo et al. investigated the electrical performance of GFRP through thermal stress testing [83]. Although some microcracks were observed in the GFRP specimens, both the AC and DC surface flashover strengths of GFRP were found to be significantly higher than those of epoxy resin. It can therefore be inferred that despite the presence of microcracks, GFRP maintains excellent electrical insulation performance under cryogenic conditions.

Damage caused by high-energy radiation is also a significant factor leading to the deterioration of material insulation performance. Li et al. investigated the electrical breakdown strength of a cyanate ester/epoxy composite at 6.1 K before and after irradiation [84]. The study found that the composite exhibited increased electrical breakdown strength at cryogenic temperatures. Furthermore, due to the presence of cyanate ester, the ^{60}Co γ-ray irradiation showed no significant impact on the electrical breakdown strength at 6.1 K, indicating that this composite system possesses excellent radiation resistance.

Due to the presence of internal microscopic defects, space charges collide with the molecular chains of the material, which can trigger the initiation of electrical treeing [85,86]. The growth behavior of electrical trees at low temperatures differs significantly from that at room temperature. Wang et al. investigated the electrical treeing characteristics of epoxy

resin at 77 K, observing carbonization in tree channels through Raman spectroscopy [87]. The study revealed that while electrical tree propagation in liquid nitrogen exhibited slower growth rates, it developed more branches with increased density and higher degrees of carbonization. The electrical trees appeared darker in color with more complex dendritic structures, indicating more severe material damage under cryogenic conditions. Notably, the electrical tree initiation probability decreased, and tree growth was significantly suppressed at low temperatures. However, once electrical trees entered the propagation phase, the size of graphitic domains within the material was found to be more than twice that observed at room temperature, which accounts for the accelerated late-stage growth of electrical trees at 77 K.

3. Conclusions

In summary, this paper presents a comprehensive and systematic review of the cryogenic performances in epoxy-based composites specifically for superconducting magnets encapsulation, including studies on cryogenic mechanical reinforcement, thermal properties enhancement, and electrical insulation characteristics. The irradiation resistance of epoxy resins in relation to these properties is also discussed. The conventional glass fiber-reinforced epoxy composites provide adequate tensile and interlaminar shear strength for current magnet systems (shown in Table 1), with excellent insulation properties. However, their low cryogenic toughness, low thermal conductivity (~0.25 W m^{-1} K^{-1} at 77 K), and relatively high thermal expansion make them insufficient for the next generation of larger fusion and accelerator magnets. An enhanced approach involves utilizing insulating ceramic nanofillers such as AlN, graphene oxide, BN, etc. This method has been demonstrated to simultaneously enhance cryogenic mechanical properties, increase thermal conductivity, and effectively reduce the thermal expansion coefficient, while maintaining excellent electrical insulation of composites. Chemical modification techniques—including the introduction of flexible segments, liquid crystals, and hyperbranched structures—can significantly enhance epoxy resin cryogenic performance. Regarding electrical insulation properties, adding inorganic fillers is one of the primary methods. However, this approach is not always beneficial and may even produce adverse effects in certain circumstances. For improving radiation resistance, utilizing hybrid-resin matrices incorporating cyanate esters or highly functionalized epoxies is proven highly effective.

In addition, several recommendations for further investigation are presented as follows:

Conduct more systematic research on the cryogenic properties of epoxy resins, elucidate the mechanisms of toughening and thermal conductivity enhancement under cryogenic conditions. Precisely establish the quantitative relationship between nanofillers and toughness/thermal property improvements of epoxy-based composites.

Apply multi-scale modeling to optimize epoxy-based composites. For example, utilize molecular dynamic simulations to design resin formulations and calculate material properties, employ macro-scale modeling and the finite element method to perform mechanical analyses on the impregnation models of superconducting coils.

Translate resin design into insulating encapsulation applications. Perform more impregnation experiments on superconducting coils with novel resin systems to assess both processability and practical performance. Combine with pore and microcrack detection techniques to identify internal defects of insulation structures.

Improve the corresponding electrical property testing equipment to delve into the mechanisms of electrical behavior under cryogenic conditions.

Targeting the future performance requirements of magnet encapsulation insulation materials, utilize a hybrid method to design advanced epoxy-based composites with synergistically enhanced properties.

Author Contributions: S.Z. and Z.M.: data collection, analysis, and writing—original draft preparation; Z.W.: writing—review and editing; R.H. and L.L.: conceptualization, writing—review and editing. All authors have read and agreed to the published version of the manuscript.

Funding: This work was supported by the Strategic Priority Research Program of the Chinese Academy of Sciences (No. XDB25040300).

Data Availability Statement: No new data were generated in this study. The data used are from previously published sources, as cited in the article.

Conflicts of Interest: The authors declare no conflicts of interest.

Abbreviations

The following abbreviations are used in this manuscript:

boron nitride nanosheet	BNNS	Hydroxyl-Terminated Hyperbranched Polyurethane	HTPU
boron nitride nanotube	BNNT	Interlaminar shear strength	ILSS
cyanate ester	CE	isopropylidenebisphenol bis[(2-glycidyloxy-3-n-butoxy)-1-propylether]	IPBE
coefficient of thermal expansion	CTE	International Thermonuclear Experimental Reactor	ITER
diethyl toluene diamine	DETDA	Liquid crystal epoxy	LCE
diglycidyl 1,2-cyclohexanedicarboxylate	DCBE	Large Hadron Collider	LHC
diglycidyl ether of bisphenol A	DGEBA	Nanodiamond	ND
diglycidyl ether of bisphenol F	DGEBF	Polyhedral oligomeric silsesquioxane	POSS
epoxy	EP	Triglycidyl p-Aminophenol	TGPAP
glass fiber-reinforced polymer	GFRP	Ultimate tensile strength	UTS
graphene oxide	GO	Vacuum-Assisted Resin Transfer Molding	VARTM
Hyperbranched polymers	HBP		
Hyperbranched poly(trimellitic anhydride-diethylene glycol) ester epoxy resin	HTDE		

References

1. Dallaev, R.; Pisarenko, T.; Papez, N.; Sadovsky, P.; Holcman, V. A Brief Overview on Epoxies in Electronics: Properties, Applications, and Modifications. *Polymers* **2023**, *15*, 3964. [CrossRef] [PubMed]
2. Plesa, I.; Notingher, P.V.; Schloegl, S.; Sumereder, C.; Muhr, M. Properties of Polymer Composites Used in High-Voltage Applications. *Polymers* **2016**, *8*, 173. [CrossRef] [PubMed]
3. Jin, F.-L.; Li, X.; Park, S.-J. Synthesis and Application of Epoxy Resins: A Review. *J. Ind. Eng. Chem.* **2015**, *29*, 1–11. [CrossRef]
4. Mohan, P. A Critical Review: The Modification, Properties, and Applications of Epoxy Resins. *Polym.-Plast. Technol. Eng.* **2013**, *52*, 107–125. [CrossRef]
5. Evans, D. Turn, Layer and Ground Insulation for Superconducting Magnets. *Phys. C Supercond.* **2001**, *354*, 136–142. [CrossRef]
6. Ma, Y.; Liu, X.; Jin, H.; Han, H.; Shi, Y.; Zhang, C.; Wu, K. Preliminary Design of Insulation System for Superconducting Conductor Testing Facility. *J. Fusion Energy* **2023**, *42*, 5. [CrossRef]
7. Feldman, J.; Stautner, W.; Kovacs, C.; Miljkovic, N.; Haran, K.S. Review of Materials for HTS Magnet Impregnation. *Supercond. Sci. Technol.* **2024**, *37*, 33001. [CrossRef]
8. Ren, Y.; Wang, F.; Chen, Z.; Chen, W. Mechanical Stability of Superconducting Magnet with Epoxy-Impregnated. *J. Supercond. Nov. Magn.* **2010**, *23*, 1589–1593. [CrossRef]
9. Rice, J.A.; Hazelton, C.S.; Fabian, P.E. Wrappable Ceramic Insulation for Superconducting Magnets. In *Advances in Cryogenic Engineering Materials: Volume 46, Part A*; Balachandran, U.B., Hartwig, K.T., Gubser, D.U., Bardos, V.A., Eds.; Springer: Boston, MA, USA, 2000; pp. 267–273. [CrossRef]
10. Schutz, J.B. Properties of Composite Materials for Cryogenic Applications. *Cryogenics* **1998**, *38*, 3–12. [CrossRef]
11. Knaster, J.; Moeslang, A.; Muroga, T. Materials Research for Fusion. *Nat. Phys.* **2016**, *12*, 424–434. [CrossRef]
12. Domun, N.; Hadavinia, H.; Zhang, T.; Sainsbury, T.; Liaghat, G.H.; Vahid, S. Improving the Fracture Toughness and the Strength of Epoxy Using Nanomaterials—A Review of the Current Status. *Nanoscale* **2015**, *7*, 10294–10329. [CrossRef] [PubMed]
13. Wetzel, B.; Rosso, P.; Haupert, F.; Friedrich, K. Epoxy Nanocomposites—Fracture and Toughening Mechanisms. *Eng. Fract. Mech.* **2006**, *73*, 2375–2398. [CrossRef]

14. Liu, D.; Wei, W.; Tang, Y.; Yong, H.; Zhou, Y. Delamination Behaviors of an Epoxy-Impregnated REBCO Pancake Coil during a Quench. *Eng. Fract. Mech.* **2023**, *281*, 109074. [CrossRef]
15. Chu, X.; Wu, Z.; Huang, C.; Huang, R.; Zhou, Y.; Li, L. ZrW2O8-Doped Epoxy as Low Thermal Expansion Insulating Materials for Superconducting Feeder System. *Cryogenics* **2012**, *52*, 638–641. [CrossRef]
16. Mohamed Mussa, M.; Sung Noh, H.; Kwon, D.; Ryu, Y.; Suk Choi, Y.; Lee, H. Thermal-Quench Behavior of Non-Insulated High-Temperature Superconducting (HTS) Racetrack Pancake Coil with Cooling Channels through the Epoxy Surface. *Results Phys.* **2021**, *24*, 104131. [CrossRef]
17. Reed, R.P.; Martovetsky, N.N. Electrical Insulation Systems for the ITER CS Modules. *AIP Conf. Proc.* **2014**, *1574*, 354–361. [CrossRef]
18. Yan, M.; Liu, L.; Chen, L.; Li, N.; Jiang, Y.; Xu, Z.; Jing, M.; Hu, Y.; Liu, L.; Zhang, X. Radiation Resistance of Carbon Fiber-Reinforced Epoxy Composites Optimized Synergistically by Carbon Nanotubes in Interface Area/Matrix. *Compos. Part B Eng.* **2019**, *172*, 447–457. [CrossRef]
19. Wu, Z.; Zhang, H.; Yang, H.; Chu, X.; Song, Y.; Wu, W.; Liu, H.; Li, L. Properties of Radiation Stable, Low Viscosity Impregnating Resin for Cryogenic Insulation System. *Cryogenics* **2011**, *51*, 229–233. [CrossRef]
20. Hemmi, T.; Nishimura, A.; Matsui, K.; Koizumi, N.; Nishijima, S.; Shikama, T. Evaluation of Inter-Laminar Shear Strength of GFRP Composed of Bonded Glass/Polyimide Tapes and Cyanate-Ester/Epoxy Blended Resin for ITER TF Coils. *AIP Conf. Proc.* **2014**, *1574*, 154–161. [CrossRef]
21. Evans, D. Resins for Superconducting Magnet Construction—An Overview of Requirements, Processing and Properties. *IOP Conf. Ser. Mater. Sci. Eng.* **2020**, *756*, 12003. [CrossRef]
22. Sathishkumar, T.; Satheeshkumar, S.; Naveen, J. Glass Fiber-Reinforced Polymer Composites—A Review. *J. Reinf. Plast. Compos.* **2014**, *33*, 1258–1275. [CrossRef]
23. Cui, M.; Mao, J.; Chen, Y.; Jin, J. Preparation, Material Modification and Cryogenic Mechanical Properties of Fiber-Reinforced Polymer (FRP) Composites. *J. Mater. Sci.* **2025**, *60*, 12222–12247. [CrossRef]
24. Paramane, A.; Awais, M.; Chandrasekaran, T.; Junaid, M.; Nazir, M.T.; Chen, X. A Review on Insulation and Dielectrics for High-Temperature Superconducting Cables for Power Distribution: Progress, Challenges, and Prospects. *IEEE Trans. Appl. Supercond.* **2023**, *33*, 4801831. [CrossRef]
25. Liu, Z.; Li, J.; Liu, X. Novel Functionalized BN Nanosheets/Epoxy Composites with Advanced Thermal Conductivity and Mechanical Properties. *ACS Appl. Mater. Interfaces* **2020**, *12*, 6503–6515. [CrossRef]
26. Qin, Y.; Zhang, S.; Han, S.; Xu, T.; Liu, C.; Xi, M.; Yu, X.; Li, N.; Wang, Z. Voltage-Stabilizer-Grafted SiO_2 Increases the Breakdown Voltage of the Cycloaliphatic Epoxy Resin. *ACS Omega* **2021**, *6*, 15523–15531. [CrossRef]
27. Wu, B.; Chen, R.; Fu, R.; Agathopoulos, S.; Su, X.; Liu, H. Low Thermal Expansion Coefficient and High Thermal Conductivity Epoxy/Al_2O_3/T-ZnOw Composites with Dual-Scale Interpenetrating Network Structure. *Compos. Part Appl. Sci. Manuf.* **2020**, *137*, 105993. [CrossRef]
28. Qu, C.-B.; Huang, Y.; Li, F.; Xiao, H.-M.; Liu, Y.; Feng, Q.-P.; Huang, G.-W.; Li, N.; Fu, S.-Y. Enhanced Cryogenic Mechanical Properties of Carbon Fiber Reinforced Epoxy Composites by Introducing Graphene Oxide. *Compos. Commun.* **2020**, *22*, 100480. [CrossRef]
29. He, Y.; Chen, Q.; Yang, S.; Lu, C.; Feng, M.; Jiang, Y.; Cao, G.; Zhang, J.; Liu, C. Micro-Crack Behavior of Carbon Fiber Reinforced Fe3O4/Graphene Oxide Modified Epoxy Composites for Cryogenic Application. *Compos. Part Appl. Sci. Manuf.* **2018**, *108*, 12–22. [CrossRef]
30. Li, J.; Wu, Z.; Huang, C.; Li, L. Gamma Irradiation Effects on Cyanate Ester/Epoxy Insulation Materials for Superconducting Magnets. *Fusion Eng. Des.* **2014**, *89*, 3112–3116. [CrossRef]
31. Huang, X.; Clayton, N.; Lu, K.; Li, G.; Wang, C.; Dai, Z.; Wang, C.; Yu, X.; Fang, L.; Liu, C.; et al. Progress of ITER Feeder System Electrical Insulation Qualification. *IEEE Trans. Appl. Supercond.* **2018**, *28*, 4202304. [CrossRef]
32. Yu, X.; Wu, W.; Pan, W.; Han, S.; Wang, L.; Wei, J.; Liu, L.; Du, S.; Zhou, Z.; Foussat, A.; et al. Development of Insulation Technology with Vacuum-Pressure-Impregnation (VPI) for ITER Correction Coil. *IEEE Trans. Appl. Supercond.* **2012**, *22*, 7700504. [CrossRef]
33. Ilyin, Y.; Farek, J.; Lorrière, P.; Bangui, G.; Man, S.; Beemsterboer, C.; Chen, Y.; Naoyuki, S.; Clayton, N.; Gung, C.-Y.; et al. Busbar System for ITER Magnets. *IEEE Trans. Appl. Supercond.* **2014**, *24*, 4701810. [CrossRef]
34. Rajak, D.K.; Pagar, D.D.; Menezes, P.L.; Linul, E. Fiber-Reinforced Polymer Composites: Manufacturing, Properties, and Applications. *Polymers* **2019**, *11*, 1667. [CrossRef] [PubMed]
35. Wu, Z.; Huang, R.; Huang, C.; Yang, Y.; Huang, X.; Li, L. Evaluation of the Cryogenic Mechanical Properties of the Insulation Material for ITER Feeder Superconducting Joint. *IOP Conf. Ser. Mater. Sci. Eng.* **2017**, *279*, 12005. [CrossRef]
36. Humer, K.; Bittner-Rohrhofer, K.; Fillunger, H.; Maix, R.K.; Prokopec, R.; Weber, H.W. Radiation Effects on the Mechanical Properties of Insulators for Fusion Magnets. *Fusion Eng. Des.* **2006**, *81*, 2433–2441. [CrossRef]

37. Humer, K.; Bittner-Rohrhofer, K.; Fillunger, H.; Maix, R.K.; Prokopec, R.; Weber, H.W. Innovative Insulation Systems for Superconducting Fusion Magnets. *Supercond. Sci. Technol.* **2006**, *19*, S96–S101. [CrossRef]
38. Wu, Z.; Li, J.; Huang, C.; Huang, R.; Li, L. Processing Characteristic and Radiation Resistance of Various Epoxy Insulation Materials for Superconducting Magnets. *Fusion Eng. Des.* **2013**, *88*, 3078–3083. [CrossRef]
39. Bao, R.; Sun, W.; Wu, Z.; Huang, C.; Li, L.; Zhou, Y. Nano Aluminum Nitride Fillers for Enhanced Mechanical and Thermal Properties of GFRP in Cryogenic Temperature Settings. *Cryogenics* **2024**, *143*, 103953. [CrossRef]
40. Gaarud, A.; Scheuerlein, C.; Parragh, D.M.; Clement, S.; Bertsch, J.; Urscheler, C.; Piccin, R.; Ravotti, F.; Pezzullo, G.; Lach, R. Fracture Toughness, Radiation Hardness, and Processibility of Polymers for Superconducting Magnets. *Polymers* **2024**, *16*, 1287. [CrossRef]
41. Haziot, A.; Kirby, G.; Dallocchio, A.; Devred, A.; Foussat, A.; Gentini, L.; Mangiarotti, F.J.; Pentella, M.; Petrone, C.; Pincot, F.-O.; et al. Curved-Canted-Cosine-Theta (CCCT) Dipole Prototype Development at CERN. *IEEE Trans. Appl. Supercond.* **2024**, *34*, 4002608. [CrossRef]
42. Mousavi, S.R.; Estaji, S.; Paydayesh, A.; Arjmand, M.; Jafari, S.H.; Nouranian, S.; Khonakdar, H.A. A Review of Recent Progress in Improving the Fracture Toughness of Epoxy-Based Composites Using Carbonaceous Nanofillers. *Polym. Compos.* **2022**, *43*, 1871–1886. [CrossRef]
43. Mousavi, S.R.; Estaji, S.; Raouf Javidi, M.; Paydayesh, A.; Khonakdar, H.A.; Arjmand, M.; Rostami, E.; Jafari, S.H. Toughening of Epoxy Resin Systems Using Core–Shell Rubber Particles: A Literature Review. *J. Mater. Sci.* **2021**, *56*, 18345–18367. [CrossRef]
44. Fan, J.; Yang, J.; Li, H.; Tian, J.; Wang, M.; Zhao, Y. Cryogenic Mechanical Properties of Graphene Oxide/Epoxy Nanocomposites: Influence of Graphene Oxide with Different Oxidation Degrees. *Polym. Test.* **2021**, *96*, 107074. [CrossRef]
45. Jin, R.; Xu, B.; Guo, D.; Qu, L. Constructing a Novel Controllable Interface Structure through the Anchoring Effect of α-Cyclodextrin at Cryogenics to Enhance and Toughen the Mechanical Properties of Epoxy Resin. *Chem. Eng. J.* **2025**, *503*, 158062. [CrossRef]
46. Yang, G.; Fu, S.-Y.; Yang, J.-P. Preparation and Mechanical Properties of Modified Epoxy Resins with Flexible Diamines. *Polymer* **2007**, *48*, 302–310. [CrossRef]
47. Mishra, K.; Gidley, D.; Singh, R.P. Influence of Self-Assembled Compliant Domains on the Polymer Network and Mechanical Properties of POSS-Epoxy Nanocomposites under Cryogenic Conditions. *Eur. Polym. J.* **2019**, *116*, 283–290. [CrossRef]
48. Wu, T.; Liu, Y.; Li, N.; Huang, G.-W.; Qu, C.-B.; Xiao, H.-M. Cryogenic Mechanical Properties of Epoxy Resin Toughened by Hydroxyl-Terminated Polyurethane. *Polym. Test.* **2019**, *74*, 45–56. [CrossRef]
49. Yang, J.-P.; Chen, Z.-K.; Yang, G.; Fu, S.-Y.; Ye, L. Simultaneous Improvements in the Cryogenic Tensile Strength, Ductility and Impact Strength of Epoxy Resins by a Hyperbranched Polymer. *Polymer* **2008**, *49*, 3168–3175. [CrossRef]
50. Zhao, Y.; Huang, R.; Wu, Z.; Zhang, H.; Zhou, Z.; Li, L.; Dong, Y.; Luo, M.; Ye, B.; Zhang, H. Effect of Free Volume on Cryogenic Mechanical Properties of Epoxy Resin Reinforced by Hyperbranched Polymers. *Mater. Des.* **2021**, *202*, 109565. [CrossRef]
51. Zhao, Y.; Wu, Z.; Guo, S.; Zhou, Z.; Miao, Z.; Xie, S.; Huang, R.; Li, L. Hyperbranched Graphene Oxide Structure-Based Epoxy Nanocomposite with Simultaneous Enhanced Mechanical Properties, Thermal Conductivity, and Superior Electrical Insulation. *Compos. Sci. Technol.* **2022**, *217*, 109082. [CrossRef]
52. Zhao, Y.; Wu, Z.; Huang, R.; Li, L.; Ma, G. Hyperbranched Boron Nitride structure-based Epoxy Composite: Simultaneous Enhancement of Mechanical Properties, Thermal Conductivity, and Superior Electrical Insulation at Cryogenic Temperatures. *Polym. Compos.* **2024**, *45*, 7967–7978. [CrossRef]
53. Elmasry, A.; Azoti, W.; El-Safty, S.A.; Elmarakbi, A. A Comparative Review of Multiscale Models for Effective Properties of Nano- and Micro-Composites. *Prog. Mater Sci.* **2023**, *132*, 101022. [CrossRef]
54. Lokanathan, M.; Acharya, P.V.; Ouroua, A.; Strank, S.M.; Hebner, R.E.; Bahadur, V. Review of Nanocomposite Dielectric Materials with High Thermal Conductivity. *Proc. IEEE* **2021**, *109*, 1364–1397. [CrossRef]
55. Su, L.; Fang, C.; Luo, H. Functionalized Montmorillonite/Epoxy Resin Nanocomposites with Enhanced Thermal and Mechanical Properties. *RSC Adv.* **2024**, *14*, 31251–31258. [CrossRef]
56. Zhou, W.; Jia, R.; Wang, N.; Cao, J.; Liang, R. Interlayer Peeling Mechanism and Electro-Magnetic-Thermal Behavior of Epoxy-Impregnated REBCO Superconducting Coils during Quench. *J. Appl. Phys.* **2025**, *137*, 133903. [CrossRef]
57. Zhu, D.-M.; Anderson, A.C. Low-Temperature Thermal Conductivity of a Glassy Epoxy-Epoxy Composite. *J. Low Temp. Phys.* **1990**, *80*, 153–160. [CrossRef]
58. Evseeva, L.; Tanaeva, S. Thermophysical Properties of Epoxy Composite-Materials at Low-Temperatures. *Cryogenics* **1995**, *35*, 277–279. [CrossRef]
59. Wu, Z.; Li, J.; Zhang, H.; Huang, R.; Li, L. Study on Thermal Properties of Radiation-Resistant Epoxy Composite. *Cryogenics* **2012**, *52*, 632–635. [CrossRef]
60. Krzak, A.; Nowak, A.J.; Frolec, J.; Králík, T.; Kotyk, M.; Boroński, D.; Matula, G. Analysis of Mechanical Properties and Thermal Conductivity of Thin-Ply Laminates in Ambient and Cryogenic Conditions. *Materials* **2024**, *17*, 5419. [CrossRef]

61. Zhang, C.; Huang, R.; Wang, Y.; Wu, Z.; Guo, S.; Zhang, H.; Li, J.; Huang, C.; Wang, W.; Li, L. Aminopropyltrimethoxysilane-Functionalized Boron Nitride Nanotube Based Epoxy Nanocomposites with Simultaneous High Thermal Conductivity and Excellent Electrical Insulation. *J. Mater. Chem. A* **2018**, *6*, 20663–20668. [CrossRef]
62. Zhou, Z.; Huang, R.; Liu, H.; Zhao, Y.; Miao, Z.; Wu, Z.; Zhao, W.; Huang, C.; Li, L. Dielectric AlN/Epoxy and SiC/Epoxy Composites with Enhanced Thermal and Dynamic Mechanical Properties at Low Temperatures. *Prog. Nat. Sci. Mater. Int.* **2022**, *32*, 304–313. [CrossRef]
63. Zhou, Z.; Wu, Z.; Liu, H.; Huang, C.; Wang, T.; Zhao, Y.; Miao, Z.; Xiang, Y.; Geng, Z.; He, F.; et al. Enhancing Cryogenic Thermal Conductivity of Epoxy Composites through the Incorporation of Boron Nitride Nanosheets/Nanodiamond Aerogels Prepared by directional-freezing Method. *Polym. Compos.* **2024**, *45*, 2670–2684. [CrossRef]
64. Xiang, Y.; Miao, Z.; Wu, Z.; Liu, H.; Huang, C.; Yang, Z.; Li, J.; Huang, R.; Li, L. Enhancing Thermal Conductivity of Epoxy-Based Composites at Low Temperatures by Si3N4 Binary Fillers. *Eur. Phys. J. Spec. Top.* **2025**, *98*, 102540. [CrossRef]
65. Li, N.; Ma, J.; Liu, Y.; Huang, G.; Qu, C.; Li, M.; Xiao, H. Investigation of Liquid Crystal Epoxy Resin Composites for Application in Cryogenic Environments. *J. Appl. Polym. Sci.* **2024**, *141*, e55631. [CrossRef]
66. ITER Physics Basis Editors; ITER Physics Expert Group Chairs and Co-Chairs; Iter Joint Central ITER Joint Central Team and Physics Unit. Chapter 1: Overview and Summary. *Nucl. Fusion* **1999**, *39*, 2137. [CrossRef]
67. Matsuda, S.; Tobita, K. Evolution of the ITER Program and Prospect for the Next-Step Fusion DEMO Reactors: Status of the Fusion Energy R&D as Ultimate Source of Energy. *J. Nucl. Sci. Technol.* **2013**, *50*, 321–345. [CrossRef]
68. Morshuis, P.H.F. Degradation of Solid Dielectrics Due to Internal Partial Discharge: Some Thoughts on Progress Made and Where to Go Now. *IEEE Trans. Dielectr. Electr. Insul.* **2005**, *12*, 905–913. [CrossRef]
69. Bartnikas, R. Partial Discharges—Their Mechanism, Detection and Measurement. *IEEE Trans. Dielectr. Electr. Insul.* **2002**, *9*, 763–808. [CrossRef]
70. Iyer, G.; Gorur, R.S.; Richert, R.; Krivda, A.; Schmidt, L.E. Dielectric Properties of Epoxy Based Nanocomposites for High Voltage Insulation. *IEEE Trans. Dielectr. Electr. Insul.* **2011**, *18*, 659–666. [CrossRef]
71. Miller, H. Surface Flashover of Insulators. *IEEE Trans. Electr. Insul.* **1989**, *24*, 765–786. [CrossRef]
72. Dissado, L.A. Understanding Electrical Trees in Solids: From Experiment to Theory. *IEEE Trans. Dielectr. Electr. Insul.* **2002**, *9*, 483–497. [CrossRef]
73. Li, Z.; Liu, J.; Ohki, Y.; Chen, G.; Gao, H.; Li, S. Surface Flashover in 50 Years: Theoretical Models and Competing Mechanisms. *High Volt.* **2023**, *8*, 853–877. [CrossRef]
74. Jiang, D.; Feng, Y.; Zhang, H.; Wu, Z.; Miao, Z.; Huang, R.; Li, L.; Zhou, Y. DC Surface Flashover Characteristics of Epoxy Resin in High Vacuum from 10 K to 299 K. *Cryogenics* **2025**, *148*, 104067. [CrossRef]
75. Jiang, D.; Geng, Z.; Miao, Z.; Huang, R.; Li, L.; Zhou, Y. Influence of Cryogenic Temperatures on DC Surface Flashover Characteristics of BNNS-Based Epoxy Nanocomposites. *Cryogenics* **2025**, *147*, 104051. [CrossRef]
76. Jiang, D.; Miao, Z.; Zhao, Y.; Geng, Z.; Xing, Y.; Huang, R.; Li, L.; Zhou, Y. Investigation on Surface Insulating Performance of Epoxy-Alumina and Epoxy-Zinc Oxide Nanocomposites at Cryogenic Temperatures. *Cryogenics* **2025**, *152*, 104196. [CrossRef]
77. Thekkethil, S.R.; Kar, S.; Rastogi, V. Multi-Physics Modelling of Quench in a Superconducting Magnet Using Bond Graph. *Phys. C Supercond. Its Appl.* **2023**, *604*, 1354179. [CrossRef]
78. Smith, R.; Niemann, R.; Kraimer, M.; Zinneman, T. Observation of Voltage Fluctuations in a Superconducting Magnet during MHD Power Generation. *IEEE Trans. Magn.* **1979**, *15*, 295–297. [CrossRef]
79. Wang, S.; Tu, Y.; Xu, S.; Qin, S.; Wu, Z.; Li, L. Electrical Performance of TGPAP and DGEBF-Based Epoxy Resin Insulation Materials for Superconducting Magnets. *Fusion Eng. Des.* **2017**, *125*, 118–122. [CrossRef]
80. Lee, Y.J.; Shin, W.J.; Lee, S.H.; Koo, J.Y.; Yoon, J.H.; Lim, K.J.; Choi, K.D.; Lee, B.W. High Voltage Dielectric Characteristics of Epoxy Nano-Composites in Liquid Nitrogen for Superconducting Equipment. *IEEE Trans. Appl. Supercond.* **2011**, *21*, 1426–1429. [CrossRef]
81. Jiang, T.; Chen, X.; Dai, C.; Guan, H.; Paramane, A. DC Breakdown and Surface Potential Behavior of Epoxy/Al_2O_3 Nanocomposites at Cryogenic Temperature. *IEEE Trans. Appl. Supercond.* **2020**, *30*, 7700707. [CrossRef]
82. Jia, P.; Huang, R.; Xu, D.; Wang, Y.; Miao, Z.; Li, L. DC Breakdown Strength of ZnO/GFRP at Room Temperature and Cryogenic Temperature. In Proceedings of the 2021 International Conference on Electrical Materials and Power Equipment (ICEMPE), Chongqing, China, 11–15 April 2021; pp. 1–4. [CrossRef]
83. Koo, J.-H.; Hwang, J.-S.; Shin, W.-J.; Sakamoto, K.; Oh, D.-H.; Lee, B.-W. Comparison of DC and AC Surface Breakdown Characteristics of GFRP and Epoxy Nanocomposites in Liquid Nitrogen. *IEEE Trans. Appl. Supercond.* **2016**, *26*, 7700804. [CrossRef]
84. Li, X.; Wu, Z.X.; Li, J.; Xu, D.; Liu, H.M.; Huang, R.J.; Li, L.F. Cryogenic Electrical Properties of Irradiated Cyanate Ester/Epoxy Insulation for Fusion Magnets. *IOP Conf. Ser. Mater. Sci. Eng.* **2017**, *279*, 12006. [CrossRef]
85. Liu, Z.; Liu, R.; Wang, H.; Liu, W. Space Charges and Initiation of Electrical Trees. *IEEE Trans. Electr. Insul.* **1989**, *24*, 83–90. [CrossRef]

86. Shimizu, N.; Laurent, C. Electrical Tree Initiation. *IEEE Trans. Dielectr. Electr. Insul.* **1998**, *5*, 651–659. [CrossRef]
87. Wang, Y.; Huang, R.; Li, C.; Zhang, C.; Shen, F.; Li, J.; Dong, H.; Zhang, H.; Zhang, H.; Li, L. Electrical Tree Characteristics of Epoxy Resin under AC Voltage at 77 K. *Cryogenics* **2019**, *99*, 123–129. [CrossRef]